

# Homology Modeling of Glycosyl Hydrolase Family 18 Enzymes and Proteins

Nathan N. Aronson,<sup>†</sup> Christopher J. Blanchard,<sup>‡</sup> and Jeffry D. Madura<sup>\*‡</sup>

Department of Biochemistry and Molecular Biology, College of Medicine, and Department of Chemistry, College of Arts and Sciences, University of South Alabama, Mobile, Alabama 36688

Received June 17, 1997<sup>®</sup>

Using state-of-the-art homology modeling methods, three-dimensional coordinates for three family 18 glycosyl hydrolases were determined. The structures for Gp39, Brp39, and chitotriosidase were computer determined using the X-ray coordinates from *SmChiA*. The results of the modeling efforts are assessed, and comparison of the modeled structures to other known family 18 members is made.

## INTRODUCTION

Chitin is a homopolysaccharide that consists of repeated *N*-acetyl- $\beta$ -(1 $\rightarrow$ 4)-D-glucosamine (Figure 1). It is extremely abundant in nature, as it is a major structural component in the exoskeleton of insects and crustaceans. Chitin is also present in mollusca, coelenterata, nematodes, protozoa, and some fungi. Next to cellulose, chitin is the most abundant polysaccharide in the biosphere. Both polysaccharides virtually form "molecular boards". They are long and flat, and this conformation is likely why nature has put them to extensive architectural use. This shape allows chitin and cellulose chains to pack closely and form exceptionally stable bundles that are held together by interchain H-bonding. Annual biological production of chitin is estimated to be 2.5 billion tons.<sup>3</sup>

Hydrolysis of chitin must also be a major metabolic process throughout the biosphere in order to balance the intense level of its biosynthesis. Thus, massive amounts of the structural polysaccharide are deposited on the ocean floor annually, but there is relatively little chitin in marine sediments. This turnover of chitin is mainly accomplished by marine bacteria using three types of polysaccharide hydrolases (glycosidases).<sup>1</sup> Each type of chitinase has a substrate specificity for the *N*-acetyl- $\beta$ -(1 $\rightarrow$ 4)-D-glucosamine bond, but they cleave at different locations along the chain (Figure 1); [1] **endochitinases** cleave internal bonds to create new substrate ends for two exochitinases: [2] **chitodextrinases** and [3] ***N*-acetyl- $\beta$ -D-hexosaminidases**. Chitodextrinase processively hydrolyzes disaccharides from the non-reducing end of soluble chitin oligosaccharides, while hexosaminidase splits the chitin disaccharides as well as hydrolyzing monosaccharides from the nonreducing end of soluble oligomers. The set of three glycosidases efficiently converts chitin to free *N*-acetylglucosamine (GlcNAc) a biological source of both carbon and nitrogen especially important in the marine environment.

Glycosidases, the general class of enzymes that hydrolyze carbohydrate polymers, have been grouped into over 50 families based on their amino acid sequence homologies.<sup>4–6</sup> Chitinases fall into family 18 and 19, while exo-hexosaminidases such as *N*-acetyl- $\beta$ -D-hexosaminidases are in a separate class (family 20). We noted important sequence homologies

between family 18 chitinases (mostly chitodextrinases) and two other types of related proteins (Table 1): [1] chitobiase, a lysosomal glycosidase that cleaves carbohydrates uniquely from the reducing-end, thereby removing either a single GlcNAc from oligosaccharides that are normally attached to asparagine-linked glycoproteins<sup>7,8</sup> or GlcNAc processively from chitin oligosaccharides and [2] chitinase-related and oviduct-specific proteins that no longer retain hydrolytic activity towards chitin or its fragments.

Glycosidases share important similarities in their reaction mechanisms, but there are variations that occur. Hen's egg white lysozyme was the first enzyme whose crystal structure was determined,<sup>9</sup> and it can act as a chitinase as well. Based on hen's egg white lysozyme, two mechanisms lead to either retention or inversion of the anomeric glycosyl bond being hydrolyzed.<sup>10,11</sup> However, the acid–base hydrolysis by lysozyme which employs two acidic amino acids within the substrate-binding groove of the active-site can vary for evolutionary forms of the enzyme that have only one acid group.<sup>12</sup>

One explanation for the similar reaction mechanism of many glycosidases is the discovery of a shared peptide folding pattern of the active-site domain for a large group of glycosidases including chitinase A from *S. marcescens* (*SmChiA*).<sup>3</sup> The general protein folding motif of these enzymes is the  $(\beta/\alpha)_8$  TIM-barrel<sup>13</sup> which consists of a cylindrical, barrel-like framework made from eight internal parallel  $\beta$ -strands that are alternately connected by eight exterior  $\alpha$ -helices. In the glycosidases this structure appropriately places in the substrate-binding groove two critical acidic residues at the correct distance above and below the glycosidic bond. Like all TIM-barrel enzymes, these two catalytic residues are located just beyond the carboxyl-ends of two of the eight  $\beta$ -strands making the  $(\beta/\alpha)_8$  barrel. Thus, evolution has led to a wide diversity of substrate specificity for hydrolysis of varied carbohydrate structures by using a few basic protein folds to provide a required disposition of identical catalytic residues.<sup>11</sup> For example, chitobiase is unique in that it hydrolyzes a reducing-end GlcNAc<sup>7</sup> while in contrast *SmChiA* processively cleaves disaccharides from the non-reducing ends of soluble chitin oligosaccharides,<sup>3</sup> a mechanism common to many exochitinases.

The chitinase-related proteins in Table 1 are especially intriguing relatives of family 18 chitinases. Homology analysis of sequences from all proteins in Table 1 indicates

\* To whom correspondence is addressed.

<sup>†</sup> College of Medicine.

<sup>‡</sup> College of Arts and Sciences.

<sup>®</sup> Abstract published in *Advance ACS Abstracts*, November 1, 1997.

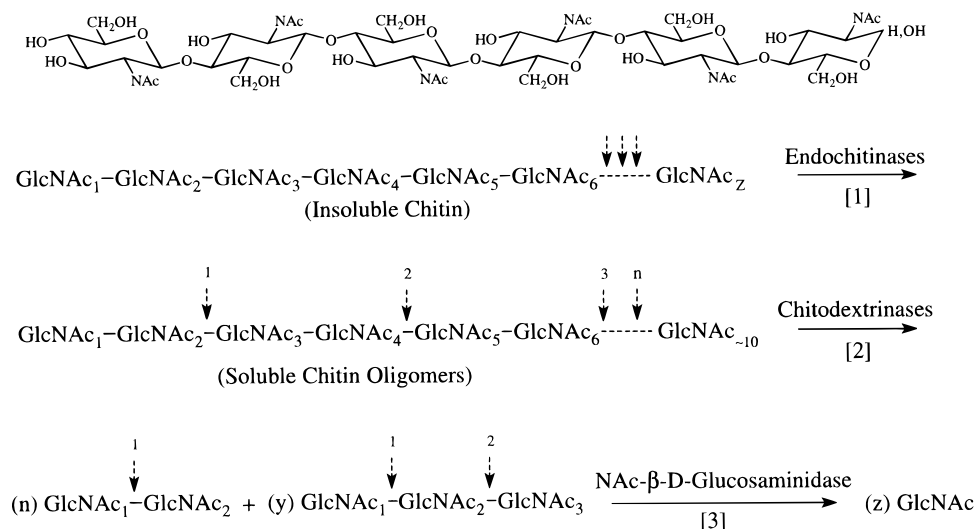


**Figure 1.** Degradation of chitin by bacterial enzymes.<sup>1</sup> A chitin hexasaccharide is depicted at the top. Each *N*-acetylglucosamine (GlcNAc) is linked  $\beta$ -1 $\rightarrow$ 4 and alternately rotated by 180°. [1] Endochitinase cleaves insoluble chitin randomly at internal bonds to release soluble oligomers of approximately 10 residues. [2] Chitodextrinase (e.g., *S. marcescens* chitinase A) progressively cleaves disaccharides from the nonreducing end of the soluble oligosaccharides with some remaining trisaccharide product ( $n \gg y$ ). [3] *N*-Acetyl- $\beta$ -D-glucosaminidase digests these di- and trisaccharides at their nonreducing ends to GlcNAc.

**Table 1.** Sequence Homologies in (I) Family 18 Chitinases; (II) Chitobiases; and (III) Chitinase-Related/Oviduct-Specific Proteins<sup>a</sup>

ENZYME/PROTEIN	$\beta$ 3	$\beta$ 4	$\beta$ 5	$\beta$ 6	$\beta$ 7	$\beta$ 8	GenBank
<b>I. Chitinases</b>							
<i>S. marcescens</i> A	267KILPSIGGWT	308DGVDIDWE	358ELTSAISAG	383DHIFLMSYD	436KIVVGTAMYGRGWT	535GLFSW	Z36294
<i>A. caviae</i>	267KILPSVGGWT	308DGVDIDWE	358ELTSAISAG	383DHIFLMSYD	436KIVVGAAMYGRGWT	535GLFAW	U09139
<i>A. sp. strain0-7</i>	265KILPSVGGWT	306DGVDIDWE	357ELTSAGAG	382DYIFAMTYD	451KLVMGVAMYGRGWE	564GLFGW	D13762
<i>B. circulans</i>	156KTLISVGGWT	197DGVLDLWE	247LLTISAGSAG	272DWINIMTYD	330KLVLGVPPFYGRGWD	429GAMFW	M57601
<i>S. pilicatus</i>	334KILYSFGGWT	376DGLDLWE	417LLTAAVTAD	445DWNVMTYD	499KLLIGIGFYGRGWT	586GAFW	M82804
<i>S. lividans</i>	333KILYSFGGWT	376DGLDLWE	417LLTAAVTAD	445DWNVMTYD	498KLLIGIGFYGRGWT	585GAFW	D12647
<i>S. thermophilaceus</i>	141KILWSFGGWT	183DG--IDWE	220LVTAATAD	248DWNVMTYD	302KLLIGIPFYGRGWT	389GAFW	D14536
<i>S. marcescens</i> B	89RIMFSIGGWY	137DGVDIDWE	180QLTIAAGAGG	207DYINLMTYD	284KIVMGVPFYGRAFK	399GVMF	X15208
<i>J. lividum</i>	360KLFISLGGWS	417DGLDLWE	467LLTAAVAG	492DWINLMTYD	548KLLIGIPFYGRGWT	643GAFW	U07025
<i>R. oligosporus</i>	105KVSLSIGGYT	146DGLDLWE	191LLTAVAPCG	216DLFYLMAYD	262KLVMGPLYGRGFC	351GAMFW	D87894
<i>S. cerevisiae</i>	175KIVMSIGGWS	216DGLDLWE	263QLSIAAPAF	288DYNNMTYD	336KLVLGMAAYGRSFH	442GGGFW	U28373
<i>K. lactis</i>	441KKIPSFSGWD	488DGLDLWE	532TLSTAIPTSS	557DYMVMTYD	604KVFVGVAAYGRSYK	703GTSW	X07127
<i>A. californica</i>	257KILPSIGGWT	298DGVLDWE	349ELTSAISAG	374KIFLMSYD	427KIVGVAMYGRGWT	524GLFAW	L22858
<i>B. mori</i>	113KILPSIGGWT	154DGVLDWE	205ELTSAISAG	230DKIFLMSYD	283KIVGVAMYGRGWT	374GLFAW	L33180
Phycodnaviridae PBCV-1	102NMHASIGGWS	145NSISLWE	194MCTIAAPEK	215DEHVMTYD	269KIFVGVAMYGRGFS	359GLVW	X42580
<i>N. tabacum</i>	92KTLPSIGGWT	134DGLDLWE	176LLTAAVSG	202DWINLMTYD	252KLVLGIPFYGRGWT	348GVFAW	X78325
<i>C. thermocellum</i>	115KTLPSIGGWT	156DGVLDWE	206LLTIAAPAG	231DFINIMTYD	288KIVGVAMYGRGWT	381GIMFW	Z68924
<i>B. malayi</i>	99KVLISYGGYN	141DGFDDLWE	181LLTAAVSG	207DLFLMSYD	261KIIIGIPMYAOGWT	358GAFW	M73689
<i>B. pahangi</i>	35KVLISYGGYN	77DGFDDLWE	117LLTAAVSG	143DLFLMSYD	197KIIIGIPMYAOGWT	294GAFW	U59690
<i>E. dispar</i>	271KVLASIGGWN	318DGLDLWE	365LLTIAAPAG	390DWINLMTYD	437KIMLGMAHYGRGWT	533GVMPW	U78318
<i>E. histolytica</i>	220KVLASIGGWN	267DGLDLWE	314LLTIAAPAG	339DWINLMTYD	386KIMLGMAHYGRGWT	482GVMPW	U78319
<i>E. invadens</i>	226QVLASIGGWN	273DGLDLWE	321LLTIAAPAG	346DWINLMTYD	393KMFVGVAMYGRGWT	489GAFW	U78320
<i>A. album</i>	123KVLMSIGGWT	164DGLDLWE	207LLSIAAPAG	232DYINLMTYD	285KIVLGMPIYGRSFO	374GTMPW	X64104
<i>T. harzianum</i>	123KVLMSIGGWT	165DGLDLWE	208LLSIAAPAG	232DYINLMTYD	286KIVLGMPIYGRSFT	375GSMFW	L14614
<i>T. hamatum</i>	124KVLMSIGGWT	165DGLDLWE	210LLSIAAPAG	235DYINLMTYD	290KIVLGMPIYGRSFE	379GSMFW	Z71415
<i>A. viteae</i>	98KILLSYGGYN	140DGFDDLWE	180LLTAAVSG	206DLFLMSYD	260KIIIGIPMYAOGWT	357GAFW	L42010
<i>A. nidulans</i>	108KVLMSIGGWT	149DGLDLWE	188QLTAVAPAG	213DFYNLMTYD	267KIIIGIPMYAOGWT	356GAMW	D87063
<i>O. volvulus</i>	98KILLSTGGYN	140DGFDDLWE	180LLTAAVSG	206DLFLMSYD	260KIIIGIPMYAOGWT	357GAFW	L42021
<i>M. sexta</i>	97KFMVAVGGWA	139DGLDLWE	182ELTAAVPLA	208DAIHVMYSYD	262KLVMGPIYGRSFT	366GAMTW	P36362
<i>Chelonius</i> sp	96KIMVAVGGWN	138DGFDDLWE	177LLSAAVAP	203DFINLMTYD	257KLVMGPIYGRSFT	355GAMW	U10422
<i>K. zopfi</i>	156KTLISVGGWT	197DGVLDLWE	247LLTISAGSAG	272DWINIMTYD	330KLVLGVPPFYGRGWD	429GAMFW	D63702
<i>V. furnissii</i>	267KILPSVGGWT	308DGVLDLWE	358ELTSAISAG	383DYIFLMSYD	436KIVVGAAMYGRGWT	535GLFAW	L42548
<i>P. japonicus</i>	116KTLNIAVGGWA	158DGLDLWE	201ELTCAVPPA	227DAIHLMTYD	282KLVMGPIYGRSFT	384GAMTW	D84250
<i>C. elegans</i>	102KTLNIAVGGWA	143DGVLDLWE	191LLSFAAGAG	217DFVNMYSYD	274KINMGPIYGRSFT	347GVMW	Z66524
<i>Coccidioides immitis</i>	123KTLISIGGWT	164DGLDLWE	207LLTISAPAG	232DFVNLMTYD	285KIFLGMPIYGRAFA	373GGGMW	L41663
<i>Chitotriosidase</i> (Human)	91KTLTIAIGGWN	133DGLDLWE	179LLSAAVAG	205DFVNLMTYD	259KLILGMPTIYGRSFT	354GAMW	U29615
<b>II. Chitobiase</b>							
Human	105KGDVSLKDI	136DGINIDIE	175QVTFDVAWS	202DFLFVMSYD	246KLVMGVPWYGYDYT	350GIGMW	M95767
Rat	90KGDVSLKDI	121DGINIDIE	160QVTFDVAWS	187DFLFVMSYD	231KLVMGIPWYGYDYI	335GIGMW	M95768
<b>III. Chitinase-Related/Oviduct-Specific (OSG) Proteins</b>							
Human gp39	91KTLISVGGWN	133DGLDLAWL	173LLSGAVSAG	199DFISIMTYD	253KLVMGIPTFGRSFT	348GAMW	M80927
Human YKL-39	90KILLSIGGYL	133DGLDVSWI	174LLTAGVSAG	200DFINLSFD	256KIVMGIPTYGRSFT	351GAMW	U49835
Mouse gp39	92KTLTIAIGGWK	134DGLDLWQ	180LLTSTGAGI	206DYIQVMTYD	260KLIVGFPAHYGHTFI	357GAVW	S27879
Mouse brp-39	92KTLISVGGWK	134DGLDLWQ	174LLSAAVSAG	200DFINLMTYD	254KLLMGIPTFGRSFT	349GAMW	X93035
Mouse ECF-L	91KTLTIAIGGWK	133DGLDLWQ	179LLTSTGAGI	205DYIQVMTYD	259KLIVGFPAHYGHTFI	356GAVW	D87757
Pig gp38	91KTLISVGGWN	133DGLDLWQ	173LLSGAVSAG	199DFISLTYD	253KLVMGIPTYGRSFT	348GAMW	U19900
<i>Drosophila</i> secreted gp	107KILLSVGGDK	158DGLDLWQ	205QPTALLRDV	231NVNSSLFYD	301KINVGATYGRPWK	395GIWSF	U13825
Human OSG	92KTLISVGGWN	134DGLDLFFL	180LLSAAVSGV	206DFINVLSDYD	255KLIMGIPTYGRFTF	351GAMW	U09550
Baboon OSG	92KTLISVGGWN	134DGLDLFFL	180LLSAAVSGV	206DFINVLSDYD	255KLIMGIPTYGRFTF	351GAMW	M59903
Mouse OSG	92KTLISVGGWN	134DGLDLFFL	180LLSAAVSGI	206DFINVLSDYD	255KLIMGIPTYGRFTF	351GAMW	D32137
Hamster OSG	71KTLISVGGWN	113DGLDLFFL	159LLSAAVSGI	185DFINVLSDYD	234KLLMGIPTYGRFTF	330GAMW	U15048
Bovine OSG	89KTLISVGGWN	131DGLDLFFL	177LLSAAVSGD	203DFISVLSDYD	252KLLMGIPTYGRFTF	348GAMW	D16639
Ovine OSG	83KTLISVGGWN	125DGLDLFFL	171LLSAAVSGD	197DFISVLSDYD	246KLLMGIPTYGRFTF	342GAMW	U17988

<sup>a</sup> The crystal structure of *S. marcescens* chitinase A has been determined to be a  $(\beta/\alpha)_8$  barrel protein.<sup>3</sup> The sequences represent strands  $\beta$ 3– $\beta$ 8 and a few adjacent amino acids. The sequences have been translated from GenBank (accession numbers indicated). The starting amino acid position of each protein segment is numbered based on the translational start methionine being residue 1.

that a common progenitor chitinase likely gave rise to these groups of proteins. However, all members of these chitinase-related groups are not active chitinases because they no longer possess the critical glutamic acid H<sup>+</sup> donor at the

carboxyl end of the fourth  $\beta$ -strand (Table 1). A logical function for these chitinase-related and oviduct-specific proteins is they retain a binding activity for chitin-like carbohydrate polymers which is important for various

developmental or remodeling processes. For example, the oviduct-specific glycoprotein appears over a few days shortly after fertilization. This protein is expressed under the influence of estrogen and its proposed role is involvement in fertilization or early cell division by the fertilized egg or its implantation in the uterus.<sup>14</sup> Human Gp39 is a major 39kDa glycoprotein secreted by articular chondrocytes and synovial fibroblasts.<sup>15</sup> It is induced in stress situations such as rheumatoid arthritis. Mouse Brp39, a "breast regression protein", is induced in mammary epithelial cells a few days after weaning.<sup>16</sup> Mammary involution involves programmed cell death, and possibly Brp39 utilizes a chitin oligosaccharide binding ability while participating in the various signal transduction pathways that lead to apoptosis of the regressing cells. Besides the unique reducing-end chitinase, a chitotriosidase<sup>17-19</sup> is the only other family 18 enzyme in humans that retains catalytic activity. This 39 kDa endo-chitinase is produced by macrophages and is found elevated in the plasma of patients with Gaucher disease.

The major goal of our research is to determine the structural biology of human lysosomal chitinase and several of these chitinase-related proteins by theoretical computer modeling. The crystal structure of a chitinase from the bacteria *Serratia marcescens* (*SmChiA*) is known,<sup>3</sup> and this enzyme is a paradigm for the modeling experiments. Computer modeling of the proteins and enzymes in Table 1 should allow us to better predict their biological function and mechanism of reaction.

#### ALIGNMENT

All of the 52 family 18 chitinase and chitinase-related proteins in Table 1 have a larger mass than heveamine, concanavalin B, narbonin, endo F<sub>1</sub>, and endo H, a separate group of this glycosidase family whose crystal structures have been determined and recently compared.<sup>20</sup> The number of amino acids comprising this latter group of smaller family 18 proteins is 273, 299, 290, 289, and 271, respectively. In contrast *S. marcescens* chitinase A has 406 residues in its chitinase domain (Table 1) which excludes an extra N-terminal domain not considered to be involved in its activity.<sup>3</sup> The major structural difference possessed by all family 18 proteins shown in Table 1 is an extra domain between the seventh and eighth  $\beta$ -strands. For all 52 proteins the number of residues making up this  $\beta$ 7 and  $\beta$ 8 insertion domain is in the very narrow range  $89 \pm 6$  amino acids. As observed in the *SmChiA* crystal structure this domain consists of a five-stranded antiparallel  $\beta$ -sheet and two helices [one being  $\alpha$ 7 of the  $(\beta/\alpha)_8$  barrel]. This region of the protein appears to make up one side of the substrate binding cleft.<sup>20</sup> In heveamine, concanavalin B, narbonin, endo F<sub>1</sub>, and endo H the number of residues between  $\beta$ 7 and  $\beta$ 8 ranges between only 21 and 31 amino acids with this sequence comprising just  $\alpha$ 7 and a small amount of loop or random coil structure. The function and importance of the extra  $\beta$ 7- $\beta$ 8 insertion domain in the 52 proteins listed in Table 1 needs to be characterized.

With few exceptions (e.g., *Aeromonas caviae* and *Alteromonas Sp*) most of the group of family 18 chitinase proteins in Table 1 differ from *SmChiA* at their N-terminal region by lacking about 40 amino acids in a loop structure between  $\beta$ 2 and  $\alpha$ 2 (residues 199-240). This missing stretch of amino acids in the sequences of the three proteins that we have modeled against *SmChiA* (Gp39, Brp39, and chitotri-

osidase) prevented the *Gap* program from the Wisconsin Sequence Analysis Package (Genetic Computer Group, Madison WI) from aligning this segment correctly and required us to adjust the computer prediction by hand (Table 2). Thus  $\beta$ 2 was easily recognized in all of these proteins by eye but was not aligned to *SmChiA* by the *Gap* program. The role of this extra loop structure in *SmChiA* and the other chitinases that possess it is not known.

#### HOMOLOGY MODELING

Once the alignment of Gp39, Brp39, and chitotriosidase with *SmChiA* had been completed, building of three-dimensional structures for these macromolecules was undertaken. All homology modeling was performed with the program LOOK which uses a method developed by M. Levitt<sup>21</sup> and is referred to as segment match modeling. The Look module SegMod takes the alignment data (Table 2) and automatically generates the three-dimensional structure using this segment match modeling. SegMod works by first breaking the target structure sequence into a set of short segments. Each segment is constructed by randomly choosing a residue which is missing at least one atom and then choosing a sufficient number of residues before and after the randomly chosen one to ensure that there are sufficient constraints to guide the matching process. Next a database of highly refined known protein X-ray structures is searched for matching segments which are then fitted onto the framework of the target structure. A matching database segment is chosen based on three criteria: The first is amino acid similarity (i.e., sequence), second is conformational similarity (i.e., structural), and third is compatibility with the target structure. In the conformational similarity evaluation the atomic coordinates of C $\alpha$  coordinates for the reference structure are used, and in the compatibility evaluation van der Waals' interactions are checked. The reference coordinates are then used to update the target structure coordinates. This process is repeated until all unknown coordinates are determined. Ten independent models are generated using this process and then averaged to obtain one final structure. This final structure is energy minimized to relieve all strain which may arise during the coordinate building and averaging phases. All of the homology modeling and energy minimizations in this paper were performed using the LOOK 2.0 software from Molecular Applications Group (Palo Alto, CA).

#### DISCUSSION

The homology modeled structures obtained from model building are illustrated in Figures 2 and 3. Each of the macromolecules is represented as a C $\alpha$  trace in both figures. Highlighted in color is the region in which there is a large "gap" of approximately 42 residues between *SmChiA* and the target proteins (see Table 2). The "active" site residues D315/E391 (based on *SmChiA* numbering) are drawn as a ball-and-stick. Figure 2 is a side view of the three macromolecules superimposed upon the reference structure *SmChiA* looking into the active site, while Figure 3 is an orthogonal view of Figure 2, looking from the top of the  $\beta$ -barrel. All of the structures are very similar, which they should be due to the high degree of sequence identity between them (see Table 3).

The first striking feature of Figure 2 is the lack of structural disruption due to the gap in the target structures as opposed





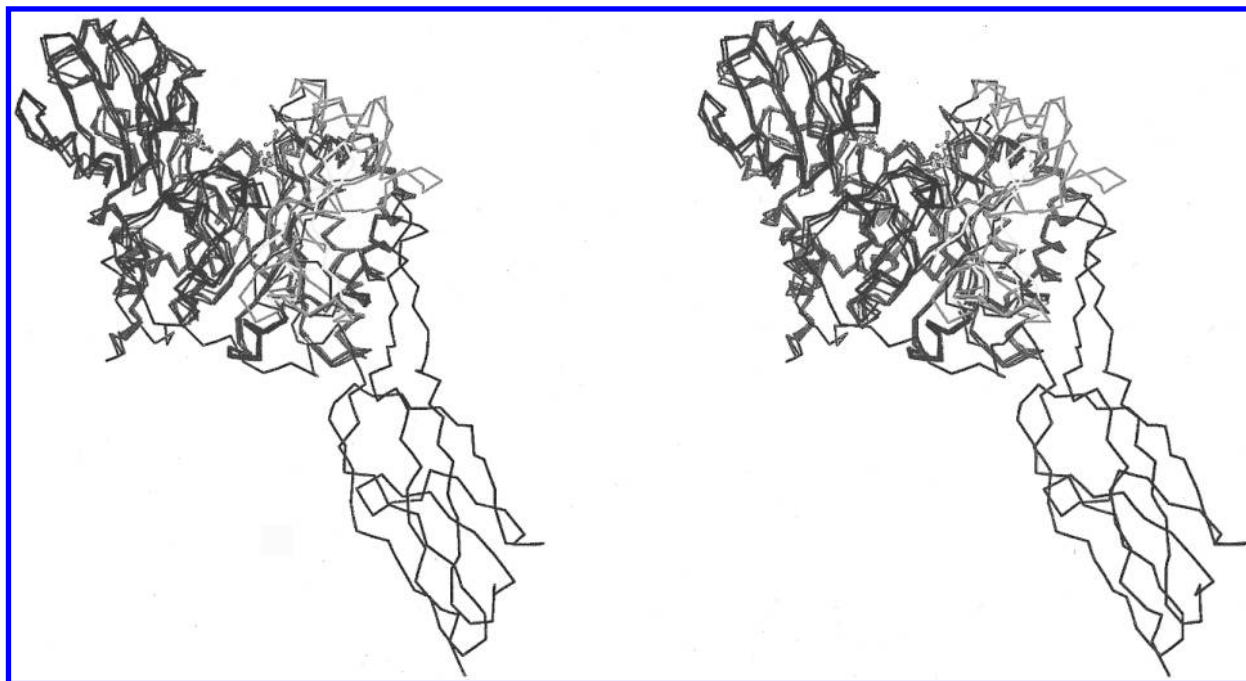


**Figure 2.**  $C_{\alpha}$  stereoview of Gp39, Brp39, chitotriosidase superimposed with *SmChiA*. This is a side view of the TIM barrel. Residues 189–259 of *SmChiA* are colored red. Residues 56–81 of Gp39, Brp39, and chitotriosidase are colored yellow, green, and blue, respectively.

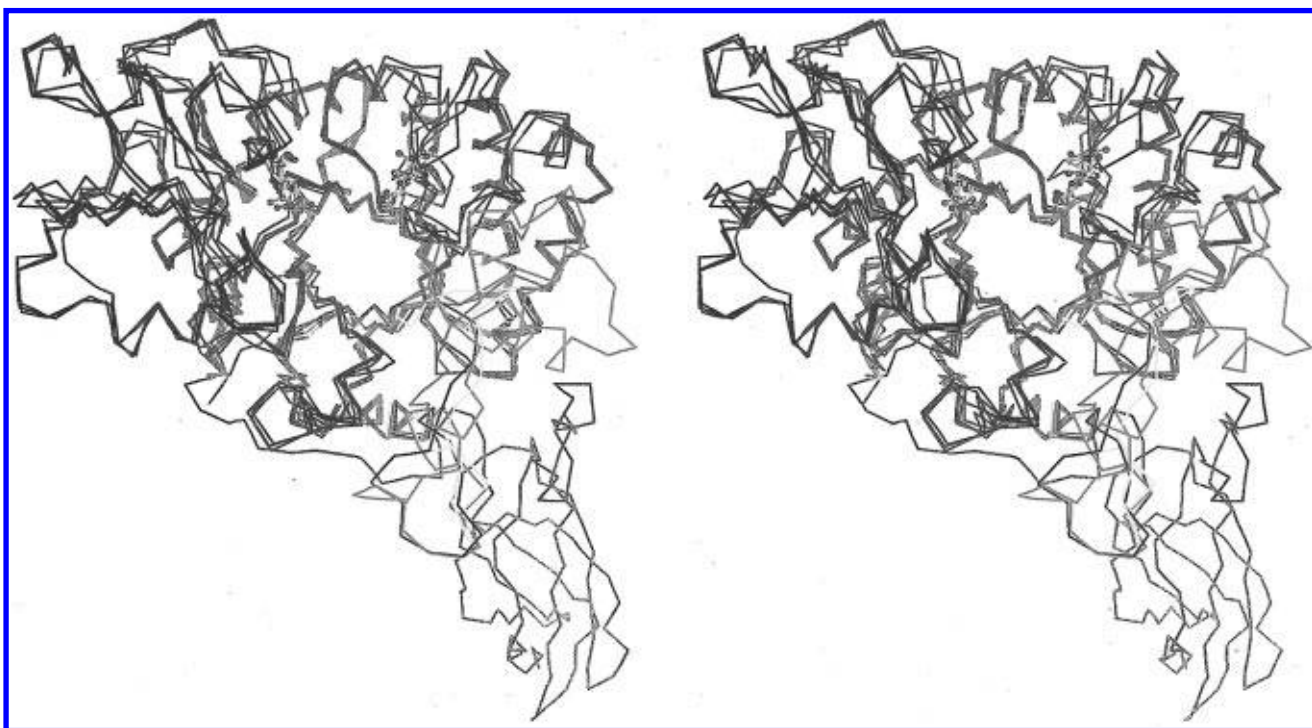


**Figure 3.**  $C_{\alpha}$  stereoview of Gp39, Brp39, chitotriosidase superimposed with *SmChiA*. This is a top view of the TIM barrel.  $\beta 1/\alpha 1$  are at the six o'clock position while  $\beta 5/\alpha 5$  are near the 12 o'clock position. The  $\beta/\alpha$  numbering proceeds counterclockwise. Residue coloring scheme is the same as that in Figure 2.

acid residue by a leucine residue. The precise mechanistic role of the  $\beta 4$  aspartate two residues in front of the proton-donor glutamate versus that of the conserved aspartate across the barrel at the end of  $\beta 6$  needs to be explained.

In *SmChiA*, narbonin, and concanavalin B, there are non-proline *cis*-peptide bonds.<sup>20</sup> In all three of the modeled structures non-proline *cis*-peptide bonds were not constructed. This is most likely due to a deficiency in LOOK.

The active site of *SmChiA* has a "wall" consisting of the  $\beta 5/\alpha 5$  loop which is part of a three-sided binding cleft. The  $\beta 5/\alpha 5$  loop in the three modeled proteins is present and presumably obstructs a bound substrate from extending beyond the +2 binding subsite.<sup>24</sup>

In a recent paper by Terwisscha et al.<sup>20</sup> they make several observations in their comparison of *SmChiA* with several other family 18 proteins. In particular they point out that phenylalanine at the end of  $\beta 2$  and the tryptophan at the end of  $\beta 8$  are near the front of the active site and may participate in substrate binding. These residues, which are conserved in all of the proteins modeled in this paper are found near the front of the active site and opposite each other. They also make note of the aspartic acid preceding  $\beta 4$  and the lysine at the beginning of  $\beta 3$ . These two residues, again highly conserved, form a salt bridge in the modeled proteins and may be there to assist in their folding. The conserved GG pair of  $\beta 3$  is close to the phenylalanine of  $\beta 2$  in all of

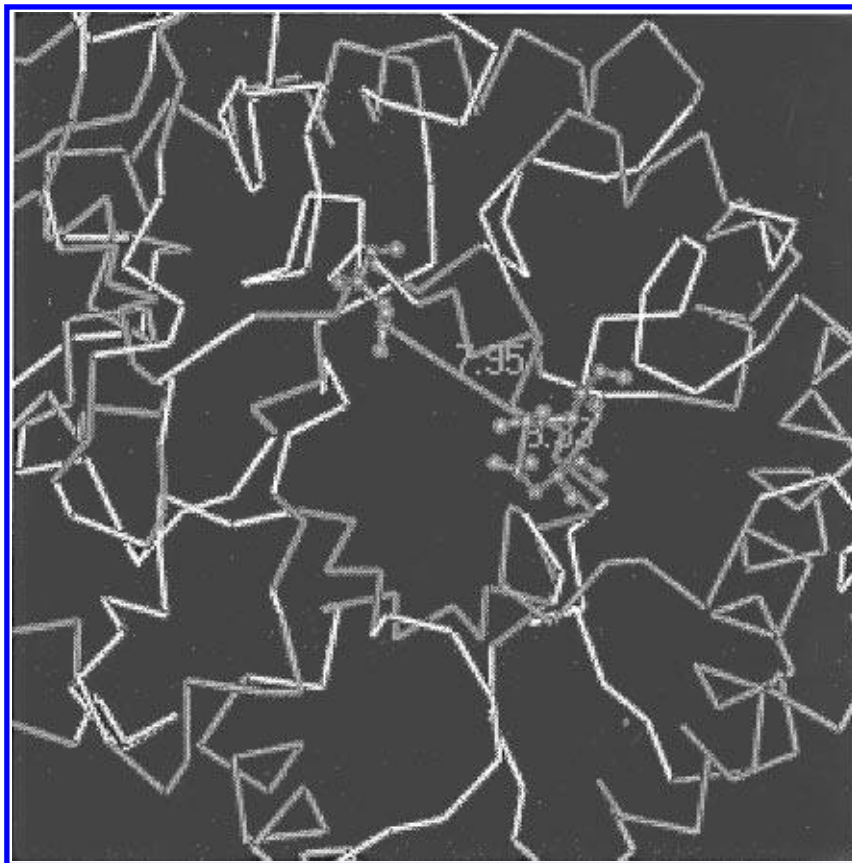


**Figure 4.** Illustrated is the C $\alpha$  trace of the active site for chitotriosidase looking down the ( $\beta/\alpha$ )<sub>8</sub> barrel. Residues D138, E140, and D213 are displayed as ball and stick models. D213 (lone residue on the left side of the active site) is 7.9 Å from residue E140.

**Table 3.** Percentage of Identical Amino Acid Residues in the Sequences of *SmChiA*, Brp39, Gp39, and Chitotriosidase<sup>a</sup>

	<i>SmChiA</i>	Chitotriosidase	Brp39	Gp39
<i>SmChiA</i>	100	28.7	26.0	28.7
Chitotriosidase		100	51.7	54.2
Brp39			100	73.8
Gp39				100

<sup>a</sup> Identical residues were found using the sequence comparison program *Gap* from Genetics Computer, Group Inc.

our modeled structures. Terwisscha et al.<sup>20</sup> suggest this GG pair is necessary to maintain the  $\beta$ -barrel due to the crowding in this region. All the other observations made by Terwisscha et al.<sup>20</sup> are consistent with our modeled structures.

We have performed a stereochemical and structural analysis on our modeled structures using the Procheck Analysis program.<sup>25</sup> According to the Procheck analysis, our current model structures have approximately 79% of their residues in the most favored region of the Ramachandran plot. As stated near the bottom of the Ramachandran plot generated by Procheck "Based on analysis of 118 structures of resolution at least 2.0 Å and *R*-factor no greater than 20%, a good quality model would be expected to have over 90% in the most favored regions".<sup>3</sup> Therefore these models are average at best. Further refinement is necessary before one can proceed to use these models in any binding studies. We are in the process of doing molecular mechanics and dynamics of these models to improve their quality. Once this has been accomplished we plan to bind substrates to these proteins and study both the binding and activity.

Overall the structures obtained from homology building appear to have similar features as other members of family 18 glycosyl hydrolases. These similarities and the results from the Procheck analysis provide some confidence that the structures built using *SmChiA* are reliable for further study until experimental coordinates become available.

## REFERENCES AND NOTES

- (1) Bassler, B. L.; Yu, C.; Lee, Y. C.; Roseman, S. Chitin Utilization by Marine Bacteria. *J. Biol. Chem.* **1991**, *266*, 24276–24286.
- (2) Jeuniaux, C.; Voss-Foucart, M. F. Chitin Biomass and Production in the Marine Environment. *Biochem. Syst. Ecol.* **1991**, *19*, 347–356.
- (3) Perrakis, A.; Tews, I.; Dauter, Z.; Oppenheim, A. B.; Chet, I.; Wilson, K. S.; Vorgias, C. E. Crystal Structure of a Bacterial Chitinase at 2.3 Å Resolution. *Structure* **1994**, *12*, 1159–1180.
- (4) Henrissat, B. A Classification of Glycosyl Hydrolases Based on Amino Acid Sequence Similarities. *Biochem. J.* **1991**, *280*, 309–316.
- (5) Henrissat, B.; Bairoch, A. New Families in the Classification of Glycosyl Hydrolases Based on Amino Acid Sequence Similarities. *Biochem. J.* **1993**, *293*, 781–788.
- (6) Henrissat, B.; Bairoch, A. Updating the Sequence Based Classification of Glycosyl Hydrolases. *Biochem. J.* **1996**, *316*, 695–696.
- (7) Aronson, N. N. Jr.; Backes, M.; Kuranda, M. J. Rat Liver Chitinase: Purification, Properties, and Role in the Lysosomal Degradation of Asn-Linked Glycoproteins. *Arch. Biochem. Biophys.* **1989**, *272*, 290–300.
- (8) Fisher, K. J.; Aronson, N. N. Jr. Cloning and Expression of the cDNA Sequence Encoding the Lysosomal Glycosidase Di-*N*-Acetylchitinase. *J. Biol. Chem.* **1992**, *267*, 19607–19616.
- (9) Phillips, D. C. The Three-dimensional Structure of an Enzyme Molecule. *Sci. Amer.* **1966**, *215*, 78–90.
- (10) Withers, S. G.; Aebersold, R. Approaches to Labelling and Identification of Active-Site Residues in Glycosidases. *Prot. Sci.* **1995**, *4*, 361–372.
- (11) Davies, G.; Henrissat, B. Structures and Mechanisms of Glycosyl Hydrolases. *Structure* **1995**, *3*, 852–859.
- (12) Matsumura, I.; Kirsch, J. F. Is Aspartate 52 Essential for Catalysis by Chicken Egg White Lysozyme? The Role of a Natural Substrate-Assisted Hydrolysis. *Biochemistry* **1996**, *35*, 1881–1889.
- (13) Reardon, D.; Farber, G. K. The Structure and Evolution of  $\alpha/\beta$  Barrel Proteins. *FASEB J.* **1995**, *9*, 497–503.

- (14) DeSouza, M. M.; Murray, M. K. An Estrogen-Dependent Secretory Protein Which Shares Identity with Chitinases, is Expressed in a Temporally and Regionally Specific Manner in the Sheep Oviduct at the Time of Fertilization and Embryo Development. *Endocrinology* **1994**, *136*, 2485–2496.
- (15) Hakala, B. E.; White, C.; Recklies, A. D. Human Cartilage Gp-39, a Major Secretory Product of Articular Chondrocytes and Synovial Cells, is a Mammalian Member of a Chitinase Protein Family. *J. Biol. Chem.* **1993**, *268*, 25803–25810.
- (16) Morrison, B. W.; Leder, P. *Neu* and *Ras* Initiate Murine Mammary Tumors that Share Genetic Markers Generally Absent in *c-myc* and *int-2*-Initiated Tumors. *Oncogene* **1994**, *9*, 3417–3426.
- (17) Hollak, C. E. M.; van Weely, S.; van Oers, M. H. J.; Aerts, J. M. F. G. Marked Elevation of Plasma Chitotriosidase Activity. *J. Clin. Invest.* **1994**, *93*, 1288–1292.
- (18) Renkema, G. H.; Boot, R. G.; Muijsers, A. O.; Donker-Koopman, W. E.; Aerts, J. M. F. G. Purification and Characterization of Human Chitotriosidase, a Novel Member of the Chitinase Family of Proteins. *J. Biol. Chem.* **1995**, *270*, 2198–2202.
- (19) Renkema, G. H.; Boot, R. G.; Strijland, A.; Donker-Koopman, W. E.; Van Den Berg, M.; Muijsers, A. O.; Aerts, J. M. F. G. Synthesis, Sorting and Processing into Distinct Isoforms of Human Macrophage Chitotriosidase. *Eur. J. Biochem.* **1997**, *244*, 279–285.
- (20) Terwisscha van Scheltinga, A. C.; Hennig, M.; Dijkstra, B. W. The 1.8 Å Resolution Structure of Hevamine, a Plant Chitinase/Lysozyme, and Analysis of the Conserved Sequence and Structure Motifs of Glycosyl Hydrolase Family 18. *J. Mol. Biol.* **1996**, *262*, 243–257.
- (21) Levitt, M. Accurate Modeling of Protein Conformation by Automatic Segment Matching. *J. Mol. Biol.* **1992**, *266*, 507–533.
- (22) Terwisscha van Scheltinga, A. C.; Armand, S.; Kalk, K. H.; Henrissat, B.; and Dijkstra, B. W. Stereochemistry of Chitin Hydrolysis by a Plant Chitinase/Lysozyme and X-ray Structure of a Complex with Allosamidin: Evidence for Substrate Assisted Catalysis. *Biochemistry* **1995**, *34*, 15619–15623.
- (23) Surles, M. C.; Richardson, J. S.; Richardson, D. C.; Brooks, F. P., Jr. Sculpting Proteins Interactively. *Prot. Sci.* **1994**, *3*, 198–210.
- (24) Davies, G. J.; Wilson, K. S.; Hennrisat, B. Nomenclature for Sugar-binding Subsites in Glycosyl Hydrolases. *Biochem. J.* **1997**, *321*, 557–559.
- (25) Lakowski, R. A.; MacArthur, M. W.; Ross, D. R.; Thornton, J. M. PROCHECK: A Program to Check the Stereochemical Quality of Protein Structures. *J. Appl. Cryst.* **1993**, *26*, 283–291.

CI970236V